

Mechanism of OH Radical Reactions with HCN and CH₃CN: OH Regeneration in the Presence of O₂

Annia Galano*

Instituto Mexicano del Petróleo, Eje Central Lázaro Cárdenas 152, 007730 México D. F., México

Received: January 31, 2007; In Final Form: March 26, 2007

A theoretical study on the mechanism of the OH reactions with HCN and CH₃CN, in the presence of O₂, is presented. Optimum geometries and frequencies have been computed at BHandHLYP/6-311++G(2d,2p) level of theory for all stationary points. Energy values have been improved by single-point calculations at the above geometries using CCSD(T)/6-311++G(2d,2p). The initial attack of OH to HCN was found to lead only to the formation of the HC(OH)N adduct, while for CH₃CN similar proportions of CH₂CN and CH₃C(OH)N are expected. A four-step mechanism has been proposed to explain the OH regeneration, experimentally observed for OH + CH₃CN reaction, when carried out in the presence of O₂. The mechanism steps are as follows: (1) OH addition to the C atom in the CN group, (2) O₂ addition to the N atom, (3) an intramolecular H migration from OH to OO, and (4) OH elimination. This mechanism is in line with the one independently proposed by Wine et al.¹¹ for HCN. The results obtained here suggest that for the OH + HCN reaction, the OH regeneration might occur even in larger extension than for OH + CH₃CN reaction. The agreement between the calculated data and the available experimental evidence on the studied reactions seems to validate the mechanism proposed here.

Introduction

Hydrogen cyanide (HCN) and acetonitrile (methyl cyanide, CH₃CN) are atmospheric tracers of biomass burning, which is considered as their main source of emission into the atmosphere.^{1,2} They are also emitted from other biogenic sources and from anthropogenic sources as well.³ Recent measurements of their concentrations in the troposphere indicate that the reactions of these compounds can be relevant to tropospheric chemistry.⁴ The major tropospheric sinks of HCN and CH₃CN are ocean uptake, scavenging by precipitation, photolysis, and reactions with OH radical.⁵ However, these are slow processes that lead to mean atmospheric residence times of several months for both cyanides. Accordingly, they travel through the troposphere and enter the stratosphere, where their lifetimes are mainly controlled by OH chemistry.

Within the temperature range relevant to atmospheric chemistry, the mechanism of CH₃CN + OH has been studied by several authors. Harris et al.⁶ studied this reaction at different temperatures and at total pressures of 100 and 500 Torr argon. They found an increase of about 18% in the rate constant at the higher pressure, which led them to conclude that the reaction proceeds partially or entirely via an addition mechanism.

On the other hand, Poulet et al.⁷ found the reaction to be pressure independent. Accordingly, they concluded that the reaction proceeds via hydrogen abstraction, leading to CH₂CN + H₂O. Kurylo and Knable⁸ also proposed the abstraction path as the primary channel of reaction, based on their finding that at 298 K the rate constant increased only about 10% when the pressure was augmented from 20 to 50 Torr. The authors found it unlikely that an addition channel in an eight-atom reaction

system would be near its high-pressure limit at 20 Torr of Ar, since such an occurrence would require that the CH₃CN–OH adduct be quite stable.

Hynes and Wine⁹ studied the CH₃CN + OH reaction by pulsed laser photolysis–pulsed laser induced fluorescence (PLP-PLIF). They suggested that two reaction paths occur in similar extension: 50% hydrogen abstraction and 50% adduct formation. They also observed regeneration of OH when the reaction was carried out in the presence of O₂. The authors proposed a mechanism to explain such regeneration, involving OH addition to the nitrogen atom, followed by O₂ addition to the –C≡N carbon atom.

More recently Tyndall et al.¹⁰ have conducted laboratory studies of the OH-radical-initiated oxidation of CH₃CN using FTIR-smog chamber techniques. They have reported the formation of formyl cyanide, HC(O)CN, with a yield of (40 ± 20)%. Implying that up to half of the OH + CH₃CN reaction could proceed via H-atom abstraction, with the remaining fraction proceeding via addition to the –C≡N group, which agrees with the results in references 6 and 9. These authors have also pointed out that the mechanism of the OH regeneration remains unexplained at present.

Concerning the HCN + OH reaction mechanism, within the temperature range relevant to atmospheric chemistry, the pressure dependence has been a controversial issue. The most recent studies on this reaction are due to Wine et al.¹¹ and Kleinbohl et al.¹² These authors have found a pressure dependence on the rate coefficient of this reaction from 10 to 600 Torr. This is in agreement with the results of Fritz et al.¹³ and contrary to the findings of Phillips.^{14,15} Works 11 and 12 deal with this reaction in the presence of O₂ and report that OH regeneration is also observed for this system. A viable mechanism has been proposed in reference 11, this time involving

* E-mail: agalano@imp.mx.

TABLE 1: Enthalpies (ΔH) and Gibbs Free Energies (ΔG) in kcal/mol, at 298.15 K, Relative to the Isolated Reactants, Corresponding to the Different Pathways Modeled for the Initial Attack of the OH Radical to R–CN Molecules

	HCN			CH ₃ CN		
	CC//BH ^a	G3	expt	CC//BH ^a	G3	expt
ΔH_{1a}^\ddagger	16.20			4.34		
ΔH_{1b}^\ddagger	3.92			3.34		
ΔH_{1c}^\ddagger	24.89			24.21		
ΔH_{1a}	9.57	9.51	6.81 ± 2.1^b	-19.99	-21.87	-24.5 ± 9.5^c
ΔH_{1b}	-22.34	-26.07		-21.71	-24.93	
ΔH_{1c}	22.75	19.37		24.90	21.53	
ΔG_{1a}^\ddagger	23.40			12.57		
ΔG_{1b}^\ddagger	11.80			12.36		
ΔG_{1c}^\ddagger	33.17			33.08		
ΔG_{1a}	8.73	8.65	6.53 ± 2.1^b	-20.90	-22.89	–
ΔG_{1b}	-13.53	-17.35		-11.67	-15.04	
ΔG_{1c}	31.45	27.98		34.46	30.92	

^a CCSD(T)//BHandHLYP/6-311++G(2d,2p). ^b From ref 31. ^c From ref 32.

OH addition to the carbon atom, followed by O₂ addition to the –C≡N nitrogen atom.

Theoretical investigations have also been performed for both reactions, but, unfortunately, they only dealt with the OH abstraction from HCN^{16–18} and CH₃CN^{18,19} and only in absence of O₂.

Even though there have been several studies on the reactions of HCN and CH₃CN with OH, the mechanism remains unclear up to date, especially when the reaction takes place in the presence of O₂. Accordingly, it is the aim of the present work to study in detail the mechanism of these gas-phase reactions and to propose a viable path that accounts for the OH regeneration. Several channels of reaction have been modeled including that proposed by Hynes and Wine.⁹

Computational Details

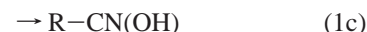
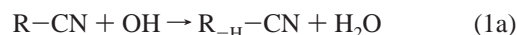
Full geometry optimizations were performed with the Gaussian 98²⁰ program using BHandHLYP hybrid functional and the 6-311++G(2d,2p) basis set. The energies of all the stationary points were improved by single-point calculations at the CCSD(T)/6-311++G(2d,2p) level of theory. This methodology known as B//A, which consists of geometry optimizations at a given level (A) followed by single-point calculations, without optimization, at a higher level (B), has become common in the study of polyatomic systems because it is relatively inexpensive from a computational point of view and it usually reproduces correctly the main features of the reaction path. It has been successfully used to describe gas-phase reactions of diverse volatile organic compounds.^{21–27} The reliability of density functional theory itself to properly describe chemical reaction has been discussed elsewhere; see, for example, refs 28–30 and references therein.

Unrestricted calculations were used for open shell systems. Frequency calculations were carried out for all the stationary points at BHandHLYP/6-311G++(2d,2p) level of theory, and local minima and transition states were identified by the number of imaginary frequencies (NIMAG = 0 or 1, respectively). Intrinsic reaction coordinate (IRC) calculations were also calculated to confirm that the transition states structures properly connect reactants and products.

Results and Discussion

Three different reaction channels have been modeled for the initial attack of the OH radical to R–CN molecules (R = –H, –CH₃): (a) the hydrogen abstraction; (b) the addition to the C

atom in the –C≡N group; and (c) the addition to the N atom (proposed by Hynes and Wine):⁹



The enthalpies (ΔH) and Gibbs free energies (ΔG) of reaction, as well as the energy barriers (ΔH^\ddagger , ΔG^\ddagger) corresponding to this first step of the reaction, relative to the isolated reactants, at 298.15 K, are reported in Table 1. The geometries of the corresponding stationary points are shown in Figure 1, where the most relevant geometrical parameters have been reported. As the data in Table 1 shows, the initial attack of OH to HCN molecule seems to occur almost exclusively as an addition to the carbon atom (channel 1b). The hydrogen abstraction reaction (channel 1a) and the addition to the nitrogen atom (channel 1c) are not only significantly endothermic ($\Delta H > 0$) and endoergic ($\Delta G > 0$) but also have higher barriers to overcome. The barriers, in terms of Gibbs free energies, of channels 1a and 1c were found to be higher than that of channel 1b by about 12 and 21 kcal/mol, respectively. These results ruled them out as viable paths for the first stage of OH + HCN reaction at room temperature and suggest that the initial attack of OH radicals to HCN molecules would lead only to the formation of the HC(OH)N adduct. These results agree with the experimental findings^{11–13} that the rate of this reaction shows a pressure dependence.

On the other hand, for OH + CH₃CN, the calculations predict channels 1a and 1b as almost equally feasible. Both Gibbs free energy barriers were found to be very similar in height: 12.6 and 12.4 kcal/mol for channels 1a and 1b, respectively. These two channels were found to be exothermic and exoergic, while channel 1c shows ΔH and ΔG values significantly above zero. According to these results, it should be expected that the initial attack of OH radicals to CH₃CN molecules would lead to the formation of CH₂CN and CH₃C(OH)N species in similar proportions. These results are supported by the reports of Hynes and Wine⁹ and Tyndall et al.,¹⁰ who proposed that up to half of the reaction could proceed via H abstraction.

In addition to the relative energies calculated at CCSD(T)//BHandHLYP/6-311++G(2d,2p) level of calculation, available experimental results have been included in Table 1, together with energy values associated with the products formation calculated at G3 level of theory. As the values in this table show, CCSD(T)//BHandHLYP/6-311++G(2d,2p) and G3 levels of

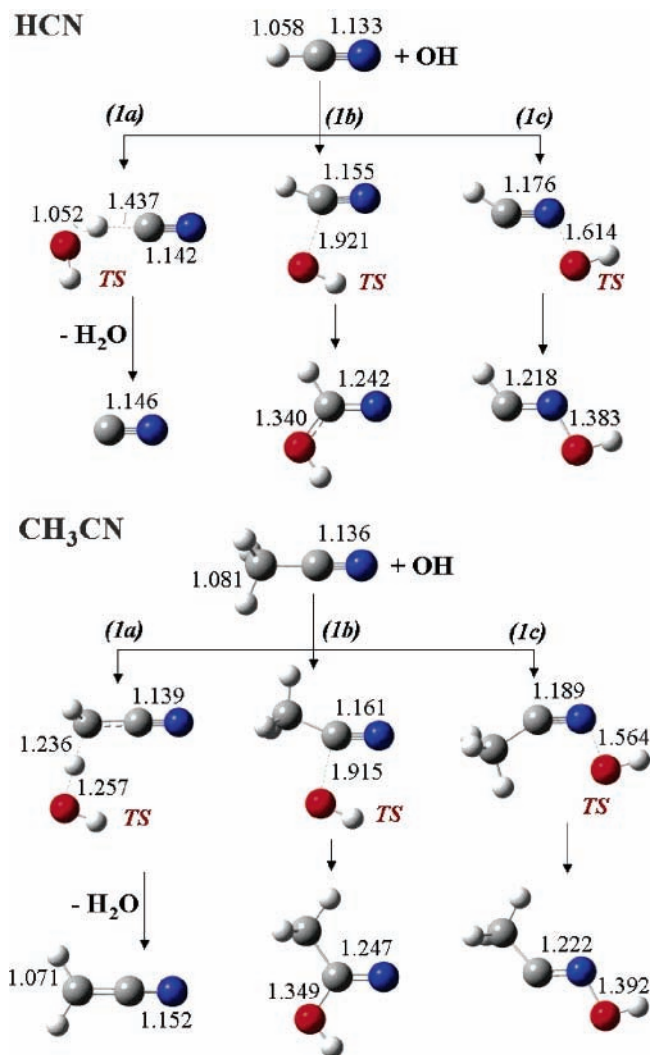


Figure 1. Different pathways modeled for the initial OH attack to HCN and CH₃CN. Geometries from BHandHLYP/6-311++G(2d,2p) calculations.

theory lead to very similar energies. From these methods the ΔH and ΔG are overestimated in 2.2 and 2.1 kcal/mol for HCN + OH reaction with respect to the experimental values, but they are almost within the range of experimental error. The calculated ΔH for the CH₃CN + OH reaction corresponds to the experimental value within the reported uncertainties for both methods. Accordingly, it seems that the CCSD(T)//BHandHLYP/6-311++G(2d,2p) method describes the studied reactions with the same accuracy as G3 and also that it reproduces the experimental behavior. Since the reliability of the calculations has been supported for this first step of the OH + R-CN reactions, it seems reasonable to trust the results obtained in the present work concerning the rest of the mechanism leading to OH regeneration in the presence of O₂.

According to the previously discussed results, the next possible step of reactions, involving O₂, would be



where channel 2b is viable for both HCN and CH₃CN (R = H and CH₃, respectively), and channel 2a would only be feasible for CH₃CN, since the OH hydrogen abstraction reaction from

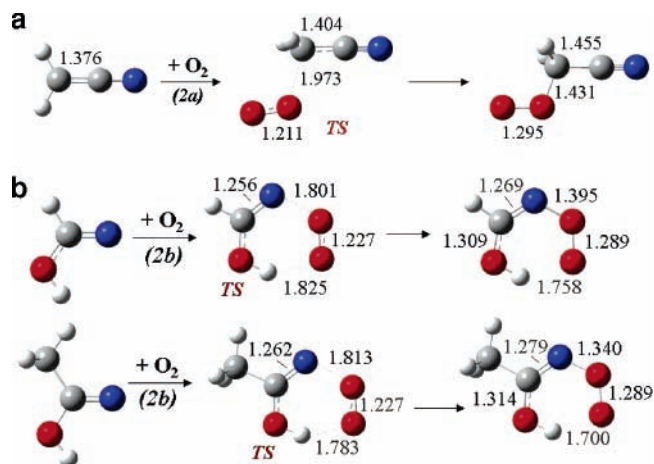


Figure 2. (a) Second step (channel 2a) of the CH₃CN + OH reaction mechanism, in presence of O₂, leading to peroxy radical formation. (b) Second step (channel 2b) of the HCN and CH₃CN + OH reaction mechanisms, leading to peroxy radical formation in the presence of O₂.

TABLE 2: Enthalpies and Gibbs Free Energies of Reaction and Barriers Corresponding to Steps of Reaction 2–4, Reported at 298.15 K^a

	HCN	CH ₃ CN		HCN	CH ₃ CN
ΔH_{2a}^\ddagger	—	5.64	ΔG_{2a}^\ddagger	—	15.18
ΔH_{2a}	—	-15.99	ΔG_{2a}	—	-5.44
ΔH_{2b}^\ddagger	8.68	7.73	ΔG_{2b}^\ddagger	19.08	18.46
ΔH_{2b}	-45.32	-47.95	ΔG_{2b}	-33.96	-36.30
ΔH_{3b}^\ddagger	2.35	1.68	ΔG_{3b}^\ddagger	3.29	2.44
ΔH_{3b}	-0.54	0.30	ΔG_{3b}	0.47	-0.22
ΔH_{4b}^\ddagger	3.83	2.60	ΔG_{4b}^\ddagger	2.07	2.19
ΔH_{4b}	-2.07	-2.33	ΔG_{4b}	-13.86	-13.09

^a All the results were obtained at CCSD(T)//BH and HLYP/6-311++G(2d,2p) level of theory.

HCN was proven to be unlikely to occur. Reaction 2a involves the addition of O₂ to the radical formed through hydrogen abstraction reaction, i.e., channel 1a. The O₂ molecule attacks the CH₂CN radical at the CH₂ site, leading to the formation of the corresponding peroxy radical (Figure 2a). This reaction was found to be exothermic and exoergic at room temperature, with ΔH of reaction about -16 kcal/mol and ΔG of reaction equal to -5.4 kcal/mol (Table 2). The barrier height was found to be equal to 15.18 and 5.64 kcal/mol, in terms of enthalpy and Gibbs free energy, respectively, which implies an entropy term of activation ($-T\Delta S^\ddagger$) of 9.5 kcal/mol.

For the fraction of the CH₃CN + OH reaction that initiates as H abstractions, and afterward follows path 2a, there is no obvious reason to expect OH regeneration. Accordingly, the subsequent fate of the peroxy radical formed as product of reaction 2a has not been modeled. In addition, it is well known that such radicals would react with NO_x, HO₂, or with other RO₂ radicals, leading to alkoxy radicals, which in turn would react with O₂.^{33,34} For CH₃CN, this last reaction would lead to the formation of HC(O)CN + HO₂.

Channel 2b (Figure 2b) represents the logical evolution of channel 1b in the presence of O₂: this molecule would attack the nitrogen end of the radical formed through the addition of OH to the carbon atom in the -CN group. In the transition states (TS), the distance of the forming N...O bond was found to be around 1.8 Å. These structures show an intramolecular hydrogen bond interaction between the H atom in the OH group and the O atom in the O₂ molecule that is directly involved in the bond formation. This intramolecular interaction, which

contributes to the stability of these species, was also found in the addition products R–C(OH)N(OO), with distances about 1.7 Å and a little shorter for CH₃CH than for HCN. It is this interaction that causes the transition states and the products of channel 2b to show ringlike structures.

As is shown in Table 2, this step (2b) is highly exoergic for both HCN and CH₃CN systems. The reaction barriers in terms of enthalpies were found to be equal to 8.68 and 7.73 kcal/mol, while in terms of Gibbs free energies are of 19.08 and 18.46 kcal/mol for HCN and CH₃CN systems, respectively. This large difference indicates that entropy is the main contributor to the thermodynamic barrier of the R–C(OH)N(OO) adduct formation. As in any addition reaction, there are usually six degrees of freedom that are affected by the formation of the adduct. Three of these are the relative translational motions of the two reactant species, and the other three are rotational degrees of freedom corresponding to their relative orientation. They are converted into six vibrations (or internal rotation) as the reaction proceeds, which causes a significant entropy loss. Accordingly, the entropies of activation ($T\Delta S^\ddagger$) were found to be relatively large: $-T\Delta S_{2b}^\ddagger$ (HCN) = 10.40 and $-T\Delta S_{2b}^\ddagger$ (CH₃CN) = 10.73 kcal/mol. Comparing this last value with $-T\Delta S_{2a}^\ddagger$ (CH₃CN), it is clear that the formation of the TS corresponding to channel 2b involves a larger entropy loss, which is a logical result taking into account that this transition state shows ringlike structure and consequently its motions are more constrained than those of TS formed in 2a.

Although the barriers ΔG_{2b}^\ddagger are relatively high, the R–C(OH)N adduct is formed with an energy excess that comes from the newly formed C–O bond. If this specie collides with a molecule of O₂, the reaction would proceed according to 2b and the R–C(OH)N(OO) radical would be formed. Assuming a 21% oxygen molecule, at least that percent of the formed R–C(OH)N would evolve in a way that leads to OH regeneration, through step 3b followed by 4b. If the R–C(OH)N adduct collides with any other molecule, and such a collision removes enough excess of energy to cause the thermal stabilization of the adduct, then the 2b step would be competing with the reverse (–1b) reaction, which would involve the break of the C–O bond and the formation of the initial R–CN and OH system. Even in that case, the system could be expected to eventually evolve through path 2b, since its barrier is about 6 kcal/mol lower than that of the reverse reaction: ΔG_{2b}^\ddagger (HCN) = 19.08, ΔG_{-1b}^\ddagger (HCN) = 25.33, ΔG_{2b}^\ddagger (CH₃CN) = 18.46, ΔG_{-1b}^\ddagger (CH₃CN) = 24.03 kcal/mol. Please notice that this comparison is fair even though path 2b is bimolecular and path –1b is unimolecular, because it has been made in terms of ΔG . These values implicate that the 2b reaction is expected to be about three orders faster than reaction –1b, for both HCN and CH₃CN. In this rough estimation it has been taken into account that reaction –1b is unimolecular and that under tropospheric conditions reaction 2b can be considered as a pseudo first-order reaction since it can be safely assumed that O₂ concentration remains constant and around 0.0086 mol/L (21%).

The proposed third step of reaction (3b, Figure 3) involves an intramolecular hydrogen migration from the OH group to the terminal O atom in the peroxy end, followed by the OH elimination (4b, Figure 4):

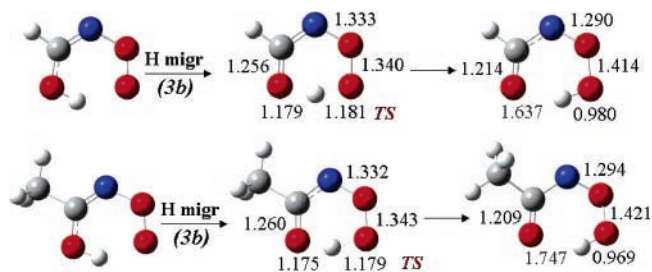
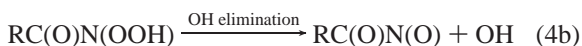
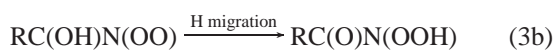


Figure 3. Third step of the proposed mechanism (channel 3b), leading to OH regeneration in the presence of O₂.

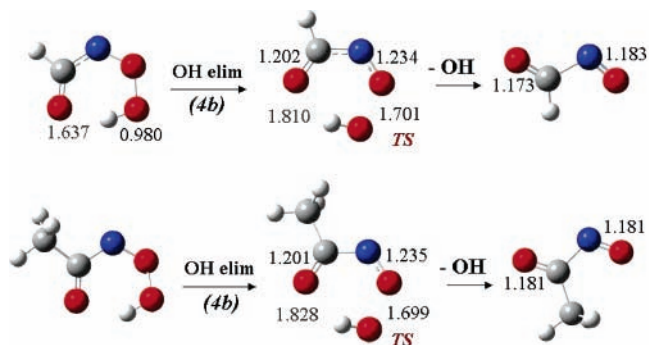


Figure 4. Fourth step of the proposed mechanism (channel 4b), leading to OH regeneration in presence of O₂.

As it can be seen in Figure 3 the geometries of the species involved in channel 3b are very similar for HCN and CH₃CN. The ringlike structure, caused by the intramolecular interaction involving the terminal H atom, is preserved in all the species. For both cyanide systems, the breaking and forming O...H bonds show very similar distances in the transition states, suggesting that the heat of reaction for this step should be near zero, since the TS structure is almost halfway between reactants and products. Another distinctive feature of this step is that the C–N–O angle decreases in the transition states compared to the corresponding reactants of products. While the 3b initial and final structures show a C–N–O angle of about 120°, for the transition states this angle was found to be equal to 116.5° and 117.2° for HCN and CH₃CN systems, respectively.

In the fourth step of reaction (4b, Figure 4) transition states show the logical shortening of C–O and N–O bonds, compared to those in products from reaction 3b. The distance of the breaking bonds were found to be about 1.7 Å, for both studied systems (R = H and R = CH₃). An intramolecular hydrogen bond was also found in this transition structure with distances about 1.8 Å between the H in the OH fragment and the O in the C=O group. The great similarity between these two TS suggest that the barriers involved in the OH elimination process should be very similar R = H and R = CH₃ systems. The final products of steps (4b) show OO *trans* conformations; even when OO *cis* structures were modeled as initial geometries of the calculations, they invariably evolved to *trans* conformations. Since based on the TS geometries it could be expected that the OO *cis* products were formed first and then eventually evolve to the *trans* conformation, IRC calculations were performed and their product ends also evolved to *trans* conformers. These results suggest that in gas phase the OO *cis* R–CONO structures are very unstable and the final products after OH elimination would exhibit OO *trans* structures.

The energy changes involved in steps 3b and 4b are very similar for both modeled systems (Table 2), as was expected from the geometries of the corresponding transition states. The heat of reaction associated with step 3b is near zero, which is

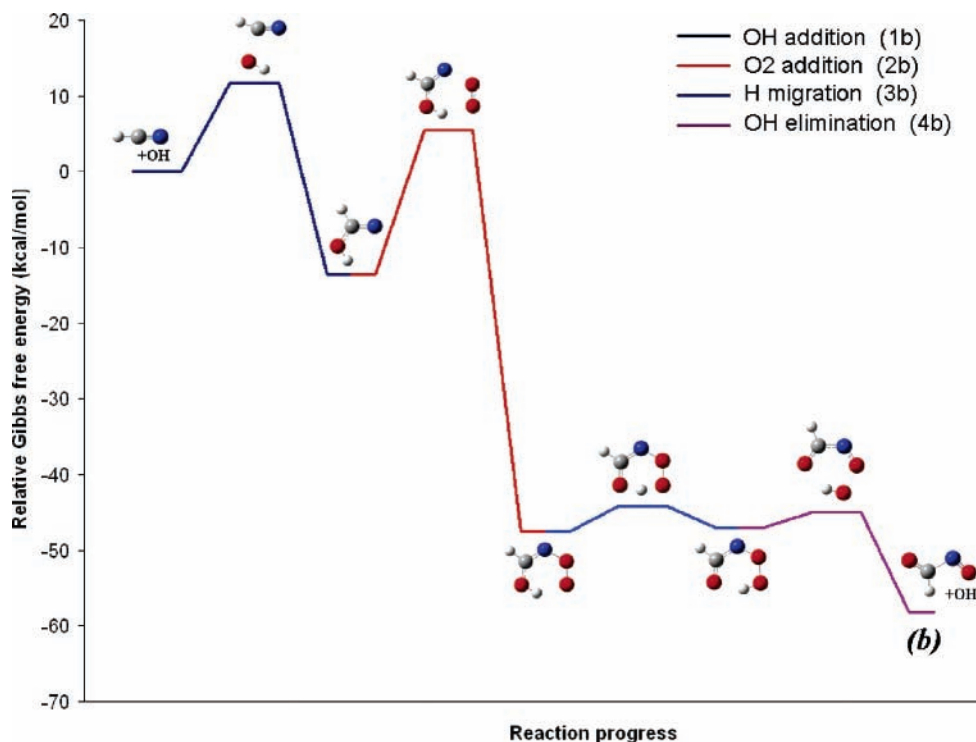


Figure 5. Reaction profiles at CCSD(T)//BHandHLYP/6-311++G(d,p) level of theory. Energies have been plotted relative to HCN + OH isolated molecules.

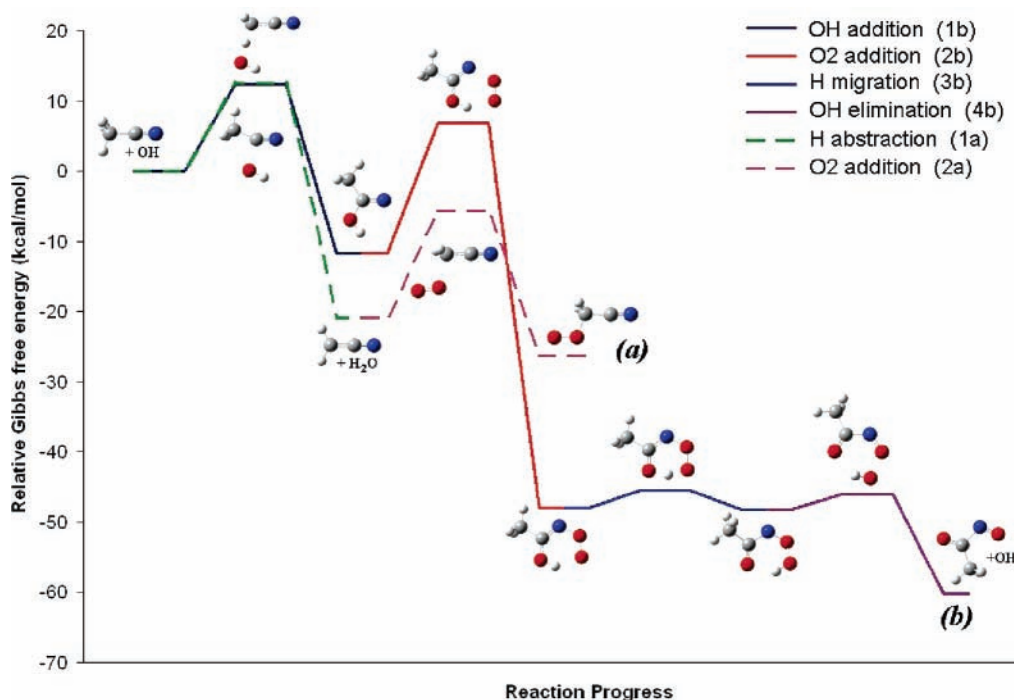


Figure 6. Reaction profiles at CCSD(T)//BHandHLYP/6-311++G(d,p) level of theory. Energies have been plotted relative to CH₃CN + OH isolated molecules.

also consistent with the transition state geometries. The enthalpies and Gibbs free energies of this step were found to be very similar, which is a logical result since no significant changes in entropy should be expected when all the involved species exhibit the same ringlike structure. On the other hand, step 4b involves a substantial entropy gain, since in the elimination reactions six vibrational modes are converted into three translational and three rotational degrees of freedom.

The 3b and 4b steps of reaction are both exoergic, and their barriers are quite low for HCN as well as for CH₃CN. Therefore,

once the RC(OH)N(OO) products are formed, it should be expected that they would promptly react through paths 3b and 4b, regenerating OH radicals. Since the products from step 2b carry a large excess of energy, and steps 3b and 4b are unimolecular, it is quite probable that the reaction proceeds through these channels before the RC(OH)N(OO) species could collide with any other molecule.

The energy profiles of the whole reactions in the presence of O₂, representing the path that was found to be more likely to occur, are shown in Figures 5 and 6. They have been plotted

using Gibbs free energy since there are addition and elimination reactions involved, thus entropy changes would be significant to the proposed mechanism. As these figures show, once the reaction starts a cascade effect could be expected, provided that the R–C(OH)CN adduct is formed with enough energy to overcome the barrier associated to step 2b. If channel 2b would not be feasible, the R–C(OH)CN adduct would accumulate and be ready to react with other reactive species, such as OH radicals. If that were the case R–C(OH)CN(OH) nonradical specie would be formed and should be observed experimentally. However, apparently there is no evidence of the formation of such specie.

The modeling performed in the present work suggests that the OH regeneration, experimentally found for the OH + CH₃CN reaction, should also be expected for OH + HCN reaction. Furthermore, a more significant OH regeneration should be expected for the OH reaction with HCN than for the reaction with methyl cyanide, provided that other conditions, including the O₂ concentration, are identical. For an O₂ concentration of 21%, characteristic of low troposphere, at least the same proportion of OH regeneration could be expected for the OH + HCN reaction and about half that amount for the OH + CH₃CN reaction. This statement is made based on the finding that while the only viable initial step for HCN is the addition to the C atom, for CH₃CN about half of the reaction is expected to take place starting by H abstraction, which would not lead to OH regeneration. Further experiments determining the extension of OH regeneration in both reactions could be very helpful to validate the mechanism proposed in this work.

Conclusions

The mechanism of OH radical with HCN and CH₃CN, in the presence of O₂, has been modeled at CCSD(T)//BHandH-LYP/6-311++G(d,p) level of theory. The calculations indicate that the initial attack of OH to HCN would only lead to the formation of the adduct HC(OH)N, while for CH₃CN the formation of the equivalent adduct and the H abstraction seem to be equally feasible. A mechanism has been proposed that accounts for the OH regeneration, experimentally observed for the OH + CH₃CN. According to the results from this work it should be expected that this regeneration also occurs for the OH + HCN reaction, even in larger extension since the only viable path for HCN initiates as OH addition to the C atom. The proposed mechanism consists on four steps, namely: (1) OH addition to the C atom in the CN group, (2) the O₂ addition to the N atom, (3) an intramolecular H migration from OH to OO, and (4) OH elimination. This proposal is in agreement with that from reference 11.

The agreement between the calculated data and the available experimental evidence on the first step of the studied reactions seems to validate the mechanism proposed here for the first time.

Acknowledgment. The author thanks the Computing Center of the Instituto Mexicano del Petróleo (IMP) for supercomputer time on SGI Origin 3000. The author also thanks the reviewers for their helpful comments.

References and Notes

(1) Lobert, J. M.; Scharffe, D. H.; Hao, W. M.; Crutzen, P. J. *Nature* **1990**, *346*, 552.
 (2) Holzinger, R.; Warneke, C.; Hansel, A.; Jordon, A.; Lindinger, W.; Scharffe, D. H.; Schade, G.; Crutzen, P. J. *Geophys. Res. Lett.* **1999**, *26*, 1161.

(3) (a) Carotti, A. A.; Kaiser, E. R. *J. Air Pollut. Control Assoc.* **1972**, *22*, 224. (b) Becker, K. H.; Ionescu, A. *Geophys. Res. Lett.* **1982**, *9*, 1349. (c) Cicerone, R. J.; Zellner, R. *J. Geophys. Res.* **1983**, *88*, 689. (d) Hamm, S.; Warneck, P. *J. Geophys. Res.* **1990**, *95*, 20593. (e) Korte, F.; Spittler, M.; Coulston, F. *Ecotoxicol. Environ. Safety* **2000**, *46*, 241.
 (4) Singh, H. B.; Salas, L.; Herlth, D.; Kolyer, R.; Czech, E.; Viezee, W.; Li, Q.; Jacob, D. J.; Blake, D.; Sachse, G.; Harward, C. N.; Fuelberg, H.; Kiley, C. M.; Zhao, Y.; Kondo, Y. *J. Geophys. Res.* **2003**, *108*, 8795.
 (5) Hamm, S.; Hahn, J.; Helas, G.; Warneck, P. *Geophys. Res. Lett.* **1984**, *11*, 1207.
 (6) Harris, G. W.; Kleindienst, T. E.; Pitts, J. N., Jr. *Chem. Phys. Lett.* **1981**, *80*, 479.
 (7) Poulet, G.; Laverdet, G.; Jourdain, J. L.; Le Bras, G. *J. Phys. Chem.* **1984**, *88*, 6259.
 (8) Kurylo, M. J.; Knable, G. L. *J. Phys. Chem.* **1984**, *88*, 3305.
 (9) Hynes, A. J.; Wine, P. H. *J. Phys. Chem.* **1991**, *95*, 1232.
 (10) Tyndall, G. S.; Orlando, J. J.; Wallington, T. J.; Hurley, M. D. *J. Phys. Chem. A* **2001**, *105*, 5380.
 (11) Wine, P. H.; Strekowski, R. S.; Nicovich, J. M.; McKee, M. L.; Kleinbohl, A.; Toon, G. C.; Sen, B.; Blavier, J.-F. L.; Weisenstein, D. K.; Wennberg, P. O. *19th International Symposium on Gas Kinetics*; Orléans, France, 2006.
 (12) Kleinbohl, A.; Toon, G. C.; Sen, B.; Blavier, J.-F. L.; Weisenstein, D. K.; Strekowski, R. S.; Nicovich, J. M.; Wine, P. H.; Wennberg, P. O. *Geophys. Res. Lett.* **2006**, *33*, L11806.
 (13) Fritz, B.; Lorenz, K.; Steinert, W.; Zellner, R. *Oxid. Commun.* **1984**, *6*, 363.
 (14) Phillips, L. F. *Chem. Phys. Lett.* **1978**, *57*, 538.
 (15) Phillips, L. F. *Aust. J. Chem.* **1979**, *32*, 2571.
 (16) Wang, C. Y.; Zhang, S. E.; Li, Q. S. *Theor. Chem. Acc.* **2002**, *108*, 341.
 (17) Palma, A.; Semprini, E.; Stefani, F.; Talamo, A. *J. Chem. Phys.* **1996**, *105*, 5091.
 (18) Li, Q. S.; Xu, X. D.; Zhang, S. *Chem. Phys. Lett.* **2004**, *384*, 20.
 (19) Li, Q. S.; Wang, C. Y. *J. Comput. Chem.* **2004**, *25*, 251.
 (20) *Gaussian 98, Revision A.3*; Frisch, M. J.; Trucks, G. W.; Schlegel, H. B.; Scuseria, G. E.; Robb, M. A.; Cheeseman, J. R.; Zakrzewski, V. G.; Montgomery, J. A., Jr.; Stratmann, R. E.; Burant, J. C.; Dapprich, S.; Millam, J. M.; Daniels, A. D.; Kudin, K. N.; Strain, M. C.; Farkas, O.; Tomasi, J.; Barone, V.; Cossi, M.; Cammi, R.; Mennucci, B.; Pomelli, C.; Adamo, C.; Clifford, S.; Ochterski, J.; Petersson, G. A.; Ayala, P. Y.; Cui, Q.; Morokuma, K.; Malick, D. K.; Rabuck, A. D.; Raghavachari, K.; Foresman, J. B.; Cioslowski, J.; Ortiz, J. V.; Stefanov, B. B.; Liu, G.; Liashenko, A.; Piskorz, P.; Komaromi, I.; Gomperts, R.; Martin, R. L.; Fox, D. J.; Keith, T.; Al-Laham, M. A.; Peng, C. Y.; Nanayakkara, A.; Gonzalez, C.; Challacombe, M.; Gill, P. M. W.; Johnson, B.; Chen, W.; Wong, M. W.; Andres, J. L.; Gonzalez, C.; Head-Gordon, M.; Replogle, E. S.; Pople, J. A. Gaussian Inc.: Pittsburgh, PA, 1998.
 (21) Mora-Diez, N.; Alvarez-Idaboy, J. R.; Boyd, R. J. *J. Phys. Chem. A* **2001**, *105*, 9034.
 (22) Alvarez-Idaboy, J. R.; Galano, A.; Bravo-Pérez, G.; Ruiz-Santoyo, Ma. E. *J. Am. Chem. Soc.* **2001**, *123*, 8387.
 (23) Galano, A.; Alvarez-Idaboy, J. R.; Bravo-Pérez, G.; Ruiz-Santoyo, Ma. E. *Phys. Chem. Chem. Phys.* **2002**, *4*, 4648.
 (24) Galano, A.; Cruz-Torres, A.; Alvarez-Idaboy, J. R. *J. Phys. Chem. A* **2006**, *110*, 1917.
 (25) Alvarez-Idaboy, J. R.; Cruz-Torres, A.; Galano, A.; Ruiz-Santoyo, Ma. E. *J. Phys. Chem. A* **2004**, *108*, 2740.
 (26) Alvarez-Idaboy, J. R.; Mora-Diez, N.; Boyd, R. J.; Vivier-Bunge, A. *J. Am. Chem. Soc.* **2001**, *123*, 2018.
 (27) Galano, A. *J. Phys. Chem. A* **2006**, *110*, 9153.
 (28) Siegbahn, P. E. M.; Blomberg, M. R. A. *Ann. Rev. Phys. Chem.* **1999**, *50*, 221.
 (29) Ziegler, T. *Chem. Rev.* **1991**, *91*, 651.
 (30) Fernandez-Ramos, A.; Miller, J. A.; Klippenstein, S. J.; Truhlar, D. G. *Chem. Rev.* **2006**, *106*, 4518.
 (31) Sander, S. P.; Friedl, R. R.; Golden, D. M.; Kurylo, M. J.; Huie, R. E.; Orkin, V. L.; Moortgat, G. K.; Ravishankara, A. R.; Kolb, E. C.; Molina, M. J.; Finlayson-Pitts, B. J. Chemical kinetics and photochemical data for use in atmospheric studies, Evaluation Number 14, JPL Publication 02-25, Pasadena, 2003.
 (32) Atkinson, R.; Baulch, D. L.; Hampson, R. F., Jr.; Kerr, J. A.; Rossi, M. J.; Troe, J. *J. Phys. Chem. Ref. Data* **1999**, *28*, 191.
 (33) Atkinson, R. *J. Phys. Chem. Ref. Data* **1994**, Monograph, 2, 1.
 (34) Aumont, B.; Szopa, S.; Madronich, S. *Atmos. Chem. Phys.* **2005**, *5*, 2497.